An Efficient Computational Strategy for Nonlinear Time History Analysis of Seismically Base-Isolated Structures

Nicolò Vaiana(✉), Salvatore Sessa, Massimo Paradiso, Francesco Marmo, and Luciano Rosati

Department of Structures for Engineering and Architecture, University of Naples Federico II, via Claudio, 21, 80124 Naples, Italy
nicolo.vaiana@unina.it

Abstract. Nonlinear time history analysis represents the most appropriate structural analysis procedure to accurately analyze seismically base-isolated structures since their dynamic response is typically governed by a system of coupled nonlinear ordinary differential equations of the second order in time. The selection of a suitable phenomenological model, required to accurately describe the hysteretic behavior of each seismic isolation bearing, as well as of a time integration method, required to numerically integrate the nonlinear equilibrium equations, plays a crucial role in performing such analyses. Indeed, both the phenomenological model and time integration method directly affect the accuracy of the results and the computational burden of the analyses. This paper proposes an efficient computational strategy obtained by combining a novel phenomenological model and an explicit structure-dependent time integration method. Numerical accuracy and computational efficiency of the proposed solution strategy are assessed by performing several nonlinear dynamic analyses on a seismically base-isolated structure and comparing the results with those obtained by employing a widely used conventional procedure.

Keywords: Phenomenological model · Time integration method · Base-isolated structure

1 Introduction

Nonlinear time history analyses are typically performed to achieve a more realistic prediction of the dynamic response of seismically base-isolated structures. The accuracy and computational efficiency of such sophisticated analyses strongly depend upon a suitable combination of the phenomenological models, adopted to describe the hysteretic behavior of the seismic isolators, and the time integration method, required to solve the nonlinear equilibrium equations [1].

A large number of uniaxial phenomenological models are available in the literature to simulate the behavior of the seismic isolation bearings. They are

A. Carcaterra et al. (Eds.): AIMETA 2019, LNME, pp. 1340–1353, 2020.
https://doi.org/10.1007/978-3-030-41057-5_108

typically divided into three main categories according to the type of equation to be solved for the evaluation of the device restoring force: (i) algebraic models [2,3], (ii) transcendental models [4,5], and (iii) differential models [6,7].

Differential models are generally adopted since they are accurate and need a relatively small number of parameters. Unfortunately, such models suffer from a limited computational efficiency due to the need of numerically solving a differential equation at each time step of the analysis; in addition, they may also require the use of sophisticated parameter identification procedures [8–11] mainly due to a somehow unclear mechanical significance of the adopted parameters.

As far as the numerical solution of the nonlinear equilibrium equations is concerned, several time integration methods are available in the literature. Such methods are usually classified into two categories according to the kind of coefficients appearing in the expressions used to compute the unknown displacement and velocity vectors at the generic time step of the analysis: (i) conventional time integration methods [12,13] and (ii) structure-dependent time integration methods [14,15].

Implicit unconditionally stable conventional time integration methods, such as the Newmark's constant average acceleration method, are currently the most widely used methods to perform nonlinear time history analyses of seismically base-isolated structures since they allow for the use of a relatively large time step, the accuracy being the only requirement to fulfill [16]; unfortunately, such methods have a limited computational efficiency and may suffer from convergence issues since they need to be used in conjunction with an iterative procedure, such as the pseudo-force method [7,17].

In this paper, we propose an accurate and computationally efficient procedure for carrying out nonlinear time history analyses of seismically base-isolated structures adopting seismic isolation devices having a kinematic hardening non-stiffening hysteretic behavior. In particular, the proposed computational strategy combines a novel phenomenological model and an explicit structure-dependent time integration method.

Compared to differential models, the proposed one does not need the numerical solution of a differential equation at each time step of the analysis for the evaluation of the device restoring force; furthermore, it is based on a set of only three parameters having a clear mechanical significance, and it can be easily implemented in a computer program.

Compared to implicit unconditionally stable conventional time integration methods, the proposed one does not require iterative procedures and, consequently, does not suffer from convergence issues. Furthermore, it is unconditionally stable for all base-isolated structures with seismic isolators having a non-stiffening hysteretic behavior, has a second-order accuracy, does not suffer from numerical damping, and displays a small relative period error for small time step.

2 Nonlinear Equilibrium Equations

The nonlinear equilibrium equations of a Multi-Degree-Of-Freedom (MDOF) system are:

$$\mathbf{M}\ddot{\mathbf{u}}(t) + \mathbf{C}\dot{\mathbf{u}}(t) + \mathbf{K}\mathbf{u}(t) + \mathbf{f}_n(t) = \mathbf{p}(t), \tag{1}$$

where $\mathbf{u}(t)$, $\dot{\mathbf{u}}(t)$, and $\ddot{\mathbf{u}}(t)$ represent the generalized displacement, velocity, and acceleration vectors, respectively, whereas $\mathbf{M}$, $\mathbf{C}$, and $\mathbf{K}$ are the generalized constant mass, damping, and elastic stiffness matrices, respectively; furthermore, $\mathbf{f}_n(t)$ represents the generalized nonlinear force vector, whereas $\mathbf{p}(t)$ is the generalized external force vector depending on time t.

Such a system of coupled nonlinear Ordinary Differential Equation (ODE) can be specialized to the structural model of a typical seismically base-isolated structure.

To this end, we introduce a three-dimensional (3D) structural model made up of two substructures, namely the n-story superstructure and the base-isolation system, as shown in Fig. 1. Its geometry is defined in a global, right-handed Cartesian coordinate system, denoted with X, Y, and Z, that is attached to the mass center of the base isolation system.

For simplicity, we assume that: (a) the superstructure deforms within its linear elastic range during the earthquake excitation; (b) each floor diaphragm is infinitely rigid in its own plane; (c) the columns are axially inextensible; (d) the beams are axially inextensible and flexurally rigid; (e) the seismic isolators are axially inextensible. Note that these assumptions, generally adopted in the literature [18], can be removed without any influence on the computational strategy proposed in this work.

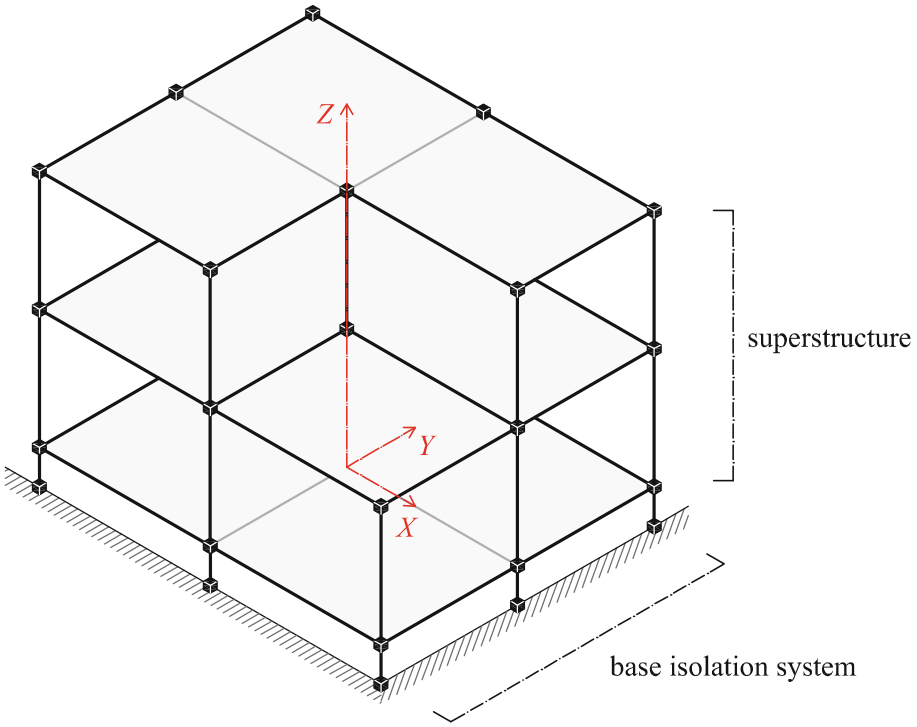

Fig. 1. 3D structural model of a typical base-isolated structure.

According to the adopted structural idealization, the displacement, velocity, and acceleration vectors of the 3D structural model, relative to the ground, may be written as:

$$\mathbf{u} = \begin{Bmatrix} \mathbf{u}_b \\ \mathbf{u}_s \end{Bmatrix}, \quad \dot{\mathbf{u}} = \begin{Bmatrix} \dot{\mathbf{u}}_b \\ \dot{\mathbf{u}}_s \end{Bmatrix}, \quad \ddot{\mathbf{u}} = \begin{Bmatrix} \ddot{\mathbf{u}}_b \\ \ddot{\mathbf{u}}_s \end{Bmatrix}, \tag{2}$$

where $\mathbf{u}_b$, $\dot{\mathbf{u}}_b$, $\ddot{\mathbf{u}}_b$ ($\mathbf{u}_s$, $\dot{\mathbf{u}}_s$, $\ddot{\mathbf{u}}_s$) represent, respectively, the displacement, velocity, and acceleration vectors of the base isolation system (superstructure), having size 3×1 ($3n \times 1$).

Consequently, the constant mass, damping, and elastic stiffness matrices become:

$$\mathbf{M} = \begin{bmatrix} \mathbf{M}_b & \mathbf{0}^T \\ \mathbf{0} & \mathbf{M}_s \end{bmatrix}, \quad \mathbf{C} = \begin{bmatrix} \mathbf{C}_b + \mathbf{C}_1 & \bar{\mathbf{C}}^T \\ \bar{\mathbf{C}} & \mathbf{C}_s \end{bmatrix}, \quad \mathbf{K} = \begin{bmatrix} \mathbf{K}_b + \mathbf{K}_1 & \bar{\mathbf{K}}^T \\ \bar{\mathbf{K}} & \mathbf{K}_s \end{bmatrix}, \tag{3}$$

where $\mathbf{M}_b$, $\mathbf{C}_b$, $\mathbf{K}_b$ ($\mathbf{M}_s$, $\mathbf{C}_s$, $\mathbf{K}_s$) are, respectively, the constant mass, damping, and elastic stiffness matrices of the base isolation system (superstructure), having size 3×3 ($3n \times 3n$), whereas matrices $\bar{\mathbf{C}}$ and $\bar{\mathbf{K}}$ are given by:

$$\bar{\mathbf{C}} = \begin{bmatrix} -\mathbf{C}_1 & \mathbf{0} \end{bmatrix}^T, \quad \bar{\mathbf{K}} = \begin{bmatrix} -\mathbf{K}_1 & \mathbf{0} \end{bmatrix}^T, \tag{4}$$

in which $\mathbf{C}_1$ and $\mathbf{K}_1$ are, respectively, the constant damping and elastic stiffness matrices of the first superstructure diaphragm, having dimension 3×3.

Finally, the nonlinear force vector and the external force vector are given by:

$$\mathbf{f}_n = \begin{Bmatrix} \mathbf{f}_{nb} \\ \mathbf{0} \end{Bmatrix}, \quad \mathbf{p} = -\begin{bmatrix} \mathbf{M}_b & \mathbf{0}^T \\ \mathbf{0} & \mathbf{M}_s \end{bmatrix} \begin{bmatrix} \mathbf{R}_b \\ \mathbf{R}_s \end{bmatrix} \ddot{\mathbf{u}}_g, \tag{5}$$

where $\mathbf{f}_{nb}$ represents the nonlinear force vector of the base isolation system, having dimension 3×1, $\mathbf{R}_b$ ($\mathbf{R}_s$) is the base isolation system (superstructure) influence matrix, having dimension 3×3 ($3n \times 3$), whereas $\ddot{\mathbf{u}}_g$ is the ground acceleration vector, having dimension 3×1.

3 Conventional Solution Strategy

In this section, a typical solution strategy, generally employed to perform Nonlinear Time History Analyses (NLTHAs) of seismically base-isolated structures, is briefly presented and the key issues affecting its efficiency are emphasized. Such a strategy combines some of the most adopted phenomenological models with a widely used time integration method, that is referred to as conventional to distinguish it from the proposed one.

3.1 Phenomenological Models

Seismic isolators can be divided into two main categories, namely *elastomeric* and *sliding bearings*. The former are made up of alternating layers of rubber and

thin reinforcing elements, whereas the latter are composed of rigid plates that can slide with respect to each other [19,20].

A large number of uniaxial phenomenological models have been proposed in the literature for simulating the complex hysteretic behavior occurring in such devices when they deform along one of their transverse directions under the effect of an axial compressive load. Depending on the kind of equation that needs to be solved for the evaluation of the device restoring force, these models can be classified into three main categories: (i) algebraic models, (ii) transcendental models, and (iii) differential models.

For the case of elastomeric bearings, the expression of the restoring force $f_j^{(i)}(t)$ of the i-th isolator of a base isolation system, along its transverse direction j, is typically defined by employing the differential model proposed by Nagarajaiah et al. [7]:

$$f_j^{(i)}(t) = aku_j^{(i)}(t) + (1-a)\,kdz_j^{(i)}(t), \tag{6}$$

where $a \in (0,1)$ is a dimensionless parameter, $k > 0$ and $d > 0$ are parameters having dimension of stiffness and displacement, respectively, and $z_j^{(i)}(t)$ is a dimensionless variable obtained by solving the following first-order nonlinear ODE:

$$\dot{z}_j^{(i)}(t) = d^{-1}\left[A\dot{u}_j^{(i)}(t) - b\left|\dot{u}_j^{(i)}(t)\right| z_j^{(i)}(t)\left|z_j^{(i)}(t)\right|^{e-1} - c\dot{u}_j^{(i)}(t)\left|z_j^{(i)}(t)\right|^{e}\right], \tag{7}$$

where e is a positive number, A, b, c are scalars, whereas $u_j^{(i)}(t)$ and $\dot{u}_j^{(i)}(t)$ are the displacement and velocity of the i-th device along its transverse direction j, respectively.

Similarly, for the case of sliding bearings, the expression of the restoring force $f_j^{(i)}(t)$ is generally defined by employing the differential model proposed by Mokha et al. [6]:

$$f_j^{(i)}(t) = \frac{N}{R}u_j^{(i)}(t) + \mu_j^{(i)}(t)Nz_j^{(i)}(t), \tag{8}$$

where N is the axial compressive force acting on the bearing, R is the radius of curvature of the sliding surface, $\mu_j^{(i)}(t)$ is the kinetic coefficient of friction, $z_j^{(i)}(t)$ is a dimensionless hysteretic variable evaluated by solving Eq. (7).

Unfortunately, the numerical solution of Eq. (7), that characterizes the celebrated Bouc-Wen model [21,22], at each time step of a NLTHA may significantly increase the overall computational effort.

3.2 Conventional Time Integration Method

The nonlinear equilibrium equations can be conveniently expressed at the generic time $t + \Delta t$:

$$\mathbf{M}\ddot{\mathbf{u}}(t+\Delta t) + \mathbf{C}\dot{\mathbf{u}}(t+\Delta t) + \mathbf{K}\mathbf{u}(t+\Delta t) + \mathbf{f}_n(t+\Delta t) = \mathbf{p}(t+\Delta t), \tag{9}$$

where Δt is the time step of a NLTHA.

Equation (9) may be numerically solved by adopting a time integration method, whose formulation is generally obtained by supplementing the equations of motion with two difference equations for the evaluation of the unknown displacement and velocity vectors. Specifically, the general formulation of a family of time integration methods can be expressed as:

$$\mathbf{M}\mathbf{a}_{i+1} + \mathbf{C}\mathbf{v}_{i+1} + \mathbf{K}\mathbf{d}_{i+1} + (\tilde{\mathbf{f}}_n)_{i+1} = \mathbf{p}_{i+1}, \tag{10a}$$

$$\mathbf{d}_{i+1} = \mathbf{d}_i + \mathbf{A}_1 \Delta t \mathbf{v}_i + \mathbf{A}_2 (\Delta t)^2 \mathbf{a}_i + \mathbf{A}_3 (\Delta t)^2 \mathbf{a}_{i+1} + \mathbf{q}_{i+1}, \tag{10b}$$

$$\mathbf{v}_{i+1} = \mathbf{v}_i + \mathbf{B}_1 \Delta t \mathbf{a}_i + \mathbf{B}_2 \Delta t \mathbf{a}_{i+1} + \mathbf{r}_{i+1}, \tag{10c}$$

where $\mathbf{d}_{i+1}$, $\mathbf{v}_{i+1}$, and $\mathbf{a}_{i+1}$ are approximate estimates of the displacement $\mathbf{u}(t+\Delta t)$, velocity $\dot{\mathbf{u}}(t+\Delta t)$, and acceleration $\ddot{\mathbf{u}}(t+\Delta t)$ vectors at the $(i+1)$-th time step, respectively; $(\tilde{\mathbf{f}}_n)_{i+1} = \mathbf{f}_n(\mathbf{d}_{i+1}, \mathbf{v}_{i+1})$ and $\mathbf{p}_{i+1}$ are approximate estimates of the nonlinear force vector $\mathbf{f}_n(t+\Delta t)$ and of the external force vector $\mathbf{p}(t+\Delta t)$ at the $(i+1)$-th time step, respectively. The matrices $\mathbf{A}_1$, $\mathbf{A}_2$, $\mathbf{A}_3$, as well as $\mathbf{B}_1$, $\mathbf{B}_2$ are coefficient matrices that define a specific family of time integration methods, whereas $\mathbf{q}_{i+1}$ and $\mathbf{r}_{i+1}$ are load-dependent vectors, namely vectors that are functions of the external force vector.

In conventional time integration methods, such as the Newmark's family of methods [12], all the coefficient matrices become scalar quantities, that is, A_1, A_2, A_3, B_1, and B_2, and both the load-dependent vectors become zero vectors, that is, $\mathbf{q}_{i+1} = \mathbf{r}_{i+1} = \mathbf{0}$.

One of the widely used conventional methods typically employed to perform NLTHAs of base-isolated structures is the Newmark's constant Average Acceleration Method (AAM), whose formulation can be obtained by setting $A_1 = 1$, $A_2 = A_3 = 1/4$, $B_1 = B_2 = 1/2$, and $\mathbf{q}_{i+1} = \mathbf{r}_{i+1} = \mathbf{0}$ in Eq. (10).

Such an implicit unconditionally stable conventional time integration method allows for the use of a relatively large time step, the accuracy being the only requirement to fulfill [16]; unfortunately, it is not computationally efficient and may suffer from convergence issues since it needs to be employed in conjunction with an iterative procedure, such as the pseudo-force method [7,17].

4 Proposed Solution Strategy

In this section, we present an alternative solution strategy that combines a novel phenomenological model with an explicit unconditionally stable time integration method. The proposed model, able to simulate the hysteretic behavior of elastomeric bearings, allows one to avoid the numerical solution of the first-order nonlinear ODE associated with the Nagarajaiah et al. Model (NM) [7]. A novel efficient model able to simulate the hysteretic behavior of sliding bearings has been already formulated by the same authors in [23]. The proposed method allows one to avoid the use of iterative procedures, such as the pseudo-force method, required when the nonlinear equilibrium equations are solved by employing the Newmark's constant average acceleration method.

4.1 Proposed Phenomenological Model

The Proposed Phenomenological Model (PPM) represents a specific instance of the more general class of uniaxial phenomenological models formulated by Vaiana et al. [24].

Figure 2 shows a restoring force-displacement hysteresis loop bounded by two parallel straight lines, typically exhibited by seismic isolators with kinematic hardening non-stiffening hysteretic behavior, obtained by imposing a sinusoidal displacement and simulated by means of the PPM.

Such a hysteresis loop can be divided into four different branches, each one corresponding to a different interval of displacement $u_j^{(i)}$ and sign of the velocity $\dot{u}_j^{(i)}$ of the i-th device along its transverse direction j. The different branches are described as follows:

- branch 1: $f_j^{(i)} = c_1 \quad \text{when} \quad x_1 \leq u_j^{(i)} < x_2 \quad \text{and } \dot{u}_j^{(i)} > 0,$
- branch 2: $f_j^{(i)} = c_2 \quad \text{when} \quad u_j^{(i)} > x_2 \text{ and } \dot{u}_j^{(i)} > 0,$
- branch 3: $f_j^{(i)} = c_3 \quad \text{when} \quad x_4 < u_j^{(i)} \leq x_3 \quad \text{and } \dot{u}_j^{(i)} < 0,$
- branch 4: $f_j^{(i)} = c_4 \quad \text{when} \quad u_j^{(i)} < x_4 \text{ and } \dot{u}_j^{(i)} < 0,$

where x_2 (x_4), representing the model history variable, is the displacement where the generic loading (unloading) curve c_1 (c_3) intersects the upper (lower) limiting curve c_2 (c_4), whereas $x_1 = x_2 - 2\bar{x}$ ($x_3 = x_4 + 2\bar{x}$). In particular, the expressions of such branches are:

$$\begin{aligned}
c_1 &= k_b u_j^{(i)} + (k_a - k_b)\left[\frac{\left(1+u_j^{(i)}-x_2+2\bar{x}\right)^{(1-\gamma)}}{1-\gamma} - \frac{(1+2\bar{x})^{(1-\gamma)}}{1-\gamma}\right] + \bar{z},\\
c_2 &= k_b u_j^{(i)} + \bar{z},\\
c_3 &= k_b u_j^{(i)} + (k_a - k_b)\left[\frac{\left(1-u_j^{(i)}+x_4+2\bar{x}\right)^{(1-\gamma)}}{\gamma-1} - \frac{(1+2\bar{x})^{(1-\gamma)}}{\gamma-1}\right] - \bar{z},\\
c_4 &= k_b u_j^{(i)} - \bar{z},
\end{aligned} \tag{11}$$

where k_a, k_b, and γ are the model parameters influencing the hysteresis loop size, whereas $\bar{x}$ and $\bar{z}$ are the internal model parameters evaluated as a function of k_a, k_b, and γ. In particular, $k_a > k_b$, $k_a > 0$, $\gamma > 0$, $\gamma \neq 1$, $\bar{x} > 0$, $\bar{z} > 0$; furthermore, the internal model parameters are computed as:

$$\bar{x} = \frac{1}{2}\left[\left(\frac{k_a - k_b}{10^{-20}}\right)^{\frac{1}{\gamma}} - 1\right], \tag{12}$$

$$\bar{z} = \frac{k_a - k_b}{2}\left[\frac{(1+2\bar{x})^{(1-\gamma)} - 1}{1-\gamma}\right], \tag{13}$$

whereas the model history variables are evaluated as:

$$x_2 = 1 + u_P + 2\bar{x} - \left\{\frac{1-\gamma}{k_a - k_b}\left[f_P - k_b u_P - \bar{z} + (k_a - k_b)\frac{(1+2\bar{x})^{(1-\gamma)}}{1-\gamma}\right]\right\}^{\left(\frac{1}{1-\gamma}\right)}, \tag{14}$$

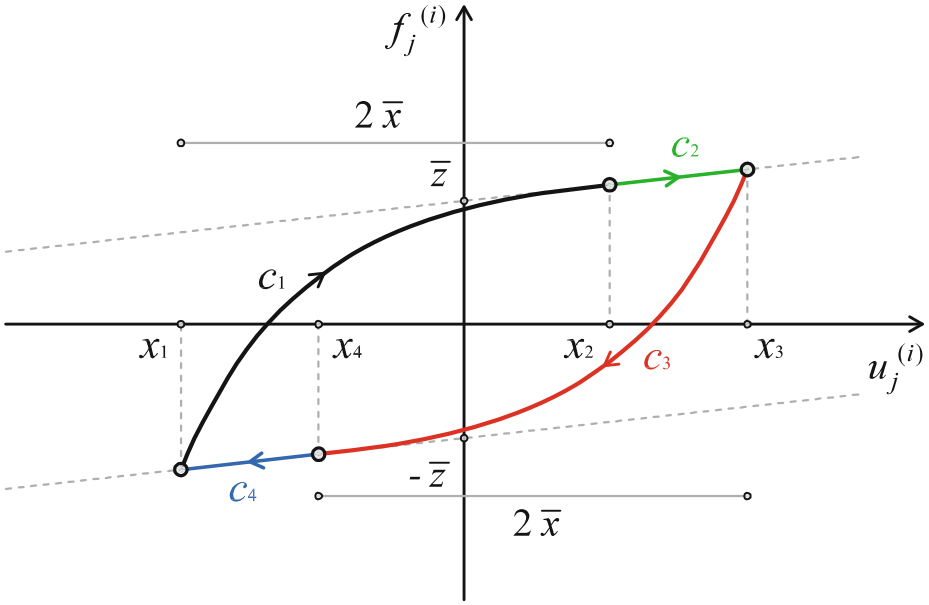

Fig. 2. Branches c_1, c_2, c_3, and c_4 for a hysteresis loop bounded by two parallel straight lines.

$$x_4 = -1+u_P-2\bar{x}+\left\{\frac{\gamma-1}{k_a-k_b}\left[f_P-k_b u_P+\bar{z}+(k_a-k_b)\,\frac{(1+2\bar{x})^{(1-\gamma)}}{\gamma-1}\right]\right\}^{\left(\frac{1}{1-\gamma}\right)}, \tag{15}$$

where (u_P,f_P) are the coordinates of the initial point P of the generic loading or unloading curve.

4.2 Proposed Explicit Time Integration Method

The Proposed Explicit Method (PEM) represents a specific algorithm of the more general family of explicit structure-dependent time integration methods developed by Chang [15], whose formulation is obtained from Eq. (10) by assuming:

$$\mathbf{A}_1 = \mathbf{1}, \quad \mathbf{A}_3 = \mathbf{0}, \quad \mathbf{B}_1 = \mathbf{A}_2, \quad \mathbf{B}_2 = \mathbf{0}, \tag{16a}$$

$$\mathbf{A}_2 = \left[\mathbf{M}+\beta\Delta t\mathbf{C}_0+\alpha(\Delta t)^2\mathbf{K}_0\right]^{-1}\mathbf{M} = \mathbf{S}_0^{-1}\mathbf{M}, \tag{16b}$$

$$\mathbf{q}_{i+1} = \mathbf{S}_0^{-1}\left[\alpha(\Delta t)^2\left(\mathbf{p}_{i+1}-\mathbf{p}_i\right)\right], \quad \mathbf{r}_{i+1} = \mathbf{0}, \tag{16c}$$

where $\mathbf{C}_0$ and $\mathbf{K}_0$ are the initial tangent damping and stiffness matrices of the base-isolated structure, respectively, and α and β are scalar parameters determining the numerical properties (i.e., accuracy and stability) of the algorithm under consideration.

The PEM, obtained by setting $\alpha = 1/4$ and $\beta = 1/2$, exhibits excellent accuracy and stability properties. Indeed, it is unconditionally stable for all non-stiffening systems, as the ones considered in this work, has a second-order

accuracy, does not suffer from numerical damping, and displays a small relative period error for small value of Δt.

As far as the PEM formulation is concerned, let us consider a generic time interval $t_i \leq t \leq t_{i+1}$ and let the external force vector $\mathbf{p}_i$ ($\mathbf{p}_{i+1}$) be assigned at the beginning (end) of the interval. We assume that the displacement, velocity, and acceleration vectors at time step i, that is, $\mathbf{d}_i$, $\mathbf{v}_i$, and $\mathbf{a}_i$, are known. Our aim is to evaluate such vectors at time step $i+1$, that is, $\mathbf{d}_{i+1}$, $\mathbf{v}_{i+1}$, and $\mathbf{a}_{i+1}$, by means of the proposed algorithm. To this end, we first observe that Eq. (10b) provides, on account of Eq. (16), the following expression for the unknown displacement vector $\mathbf{d}_{i+1}$:

$$\mathbf{d}_{i+1} = \mathbf{d}_i + \Delta t \mathbf{v}_i + \mathbf{S}_0^{-1} \left[\mathbf{M}(\Delta t)^2 \mathbf{a}_i + \alpha (\Delta t)^2 \left(\mathbf{p}_{i+1} - \mathbf{p}_i \right) \right]. \tag{17}$$

The unknown velocity vector $\mathbf{v}_{i+1}$ can be computed by using Eq. (10c) that, on account of Eq. (16), can be also written as:

$$\mathbf{v}_{i+1} = \mathbf{v}_i + \mathbf{S}_0^{-1} \mathbf{M} \Delta t \mathbf{a}_i. \tag{18}$$

Once the nonlinear forces vector $(\tilde{\mathbf{f}}_n)_{i+1} = \mathbf{f}_n(\mathbf{d}_{i+1}, \mathbf{v}_{i+1})$ has been evaluated by employing suitable phenomenological models, the unknown acceleration vector $\mathbf{a}_{i+1}$ can be computed by using the following expression derived from Eq. (10a):

$$\mathbf{a}_{i+1} = \mathbf{M}^{-1} \left[\mathbf{p}_{i+1} - \mathbf{C}\mathbf{v}_{i+1} - \mathbf{K}\mathbf{d}_{i+1} - (\tilde{\mathbf{f}}_n)_{i+1} \right]. \tag{19}$$

5 Numerical Experiments

This section presents the results of several analyses carried out on a seismically base-isolated structure, subjected to bidirectional earthquake excitation, in order to investigate the accuracy and the computational efficiency of the proposed procedure.

To perform the analyses, the proposed phenomenological model, described in 4.1, is used to reproduce the dynamic behavior of each elastomeric bearing adopted in the base isolation system of the analyzed structure. Furthermore, the proposed explicit time integration method, described in 4.2, is employed to numerically integrate the nonlinear equilibrium equations.

In order to demonstrate the accuracy properties of the proposed procedure and its capability to significantly decrease the computational burden of the analyses, the numerical results and the computational times are compared with those obtained by employing the conventional solution strategy described in Sect. 3; such a strategy combines the differential model proposed by Nagarajaiah et al. [7] with the well-known Newmark's constant average acceleration method [12].

Note that, in this paper, the first-order nonlinear ODE, characterizing the above-mentioned differential model and given by Eq. (7), is numerically solved by using the unconditionally stable semi-implicit Runge-Kutta method [25] and considering 50 steps. Furthermore, the Newmark's constant average acceleration

method is adopted in conjunction with the pseudo-force iterative procedure in which a convergence tolerance value of 10^{-8} has been assumed.

The hysteretic models and the solution algorithms have been programmed in MATLAB and run on a computer having an Intel®Core^{TM}i7-4700MQ processor and a CPU at 2.40 GHz with 16 GB of RAM.

5.1 Base-Isolated Structure Properties

Fig. 1 shows the 3D structural model of the seismically base-isolated structure selected to carry out the numerical experiments. In particular, the superstructure is a two-story reinforced concrete structure with vertical geometric irregularity, plan dimension along the X-axis (Y-axis) equal to 10 m (8 m), and story height of 3.5 m. The weight of the superstructure is 1802.9 kN and the first three natural periods are $T_{s1} = 0.15$ s, $T_{s2} = 0.14$ s, and $T_{s3} = 0.10$ s, respectively. As a result of the assumptions made in Sect. 2, the total number of the superstructure DOFs is equal to 6.

The base isolation system, having a total weight of 914.9 kN, consists of 9 elastomeric bearings, namely lead rubber bearings, that are placed under the superstructure columns, and a full diaphragm above the isolation devices. Because of the assumptions detailed in Sect. 2, the total number of the base isolation system DOFs is equal to 3. Note that the base isolation system has been designed in order to provide an effective isolation period $T_{eff} = 2.25$ s and an effective viscous damping $\zeta_{eff} = 0.15$ at the design displacement $D_d = 0.50$ m.

5.2 Applied Earthquake Excitation

The analyses are performed by imposing, along the X-axis (Y-axis), the component SN (SP) of the 1994 Northridge motion, and by adopting a ground acceleration record time step of 0.0025 s.

5.3 Hysteretic Models Parameters

The dynamic behavior of the elastomeric bearings is simulated adopting the novel phenomenological model, presented in 4.1, when the analysis is carried out by employing the proposed procedure; on the contrary, it is modeled by means of the Nagarajaiah et al. model, described in 3.1, when the analysis is performed by using the conventional procedure. Specifically, the parameters adopted in each hysteretic model are listed in Table 1.

5.4 Numerical Results

The results of the analyses carried out on the analyzed base-isolated structure are shown in Table 2. The accuracy of the Proposed Procedure (PP) is very satisfactory since the maximum and minimum values of the displacement of the base isolation system mass center along the X (Y) direction, that is, $u_x^{(MC_b)}$

Table 1. Hysteretic models parameters.

NM	$k\,[\mathrm{Nm}^{-1}]$	a	b	c	$d\,[\mathrm{m}]$	e	A
	1.834×10^6	0.10	1	0	0.0171	1.1	1
PPM	$k_a\,[\mathrm{Nm}^{-1}]$	$k_b\,[\mathrm{Nm}^{-1}]$	γ				
	3.669×10^6	1.834×10^5	62.5				

Table 2. Nonlinear time history analyses results.

			$u_x^{(MC_b)}$ [m]		$u_y^{(MC_b)}$ [m]		$\ddot{u}_x^{(MC_2)}$ [g]		$\ddot{u}_y^{(MC_2)}$ [g]	
	tct [s]	*tctp*	Max	Min	Max	Min	Max	Min	Max	Min
CP	2051.80	–	0.25	−0.24	0.26	−0.20	0.45	−0.38	1.22	−1.10
PP	3.13	0.15%	0.25	−0.24	0.26	−0.20	0.46	−0.38	1.24	−1.11

($u_y^{(MC_b)}$), as well as the ones of the acceleration of the second story mass center along the X (Y) direction, that is, $\ddot{u}_x^{(MC_2)}$ ($\ddot{u}_y^{(MC_2)}$), are numerically quite close to those predicted by using the Conventional Procedure (CP).

Figure 3a (b) shows the restoring force-displacement hysteresis loops displayed along the X (Y) direction by the isolator having coordinates $X = -5$ m and $Y = 4$ m, referred to as Isolator 1. Generally speaking, the comparison between the responses of the analyzed structure obtained with the PP and the CP shows a very good agreement.

In order to show the computational efficiency of the proposed strategy, Table 2 presents the average total computational time *tct* required to analyze the structure by employing the PP and the CP. It is evident that the computational burden of the proposed procedure, expressed by *tct*, is significantly reduced with respect to that characterizing the conventional one.

We also report a second parameter, denominated *tctp*, since the parameter *tct* is not a fully objective measure of the PP efficiency due to its dependency on the amount of the back-ground process running on the computer, the relevant memory, as well as the CPU speed. In particular, the parameter *tctp* has been obtained by normalizing the *tct* parameter of the proposed approach with respect to that characterizing the conventional one. Hence, by defining:

$$\text{PP } tctp\ [\%] = \frac{\text{PP } tct}{\text{CP } tct} \cdot 100\ , \tag{20}$$

one obtains a more meaningful measure of the computational benefits related to the use of the proposed strategy.

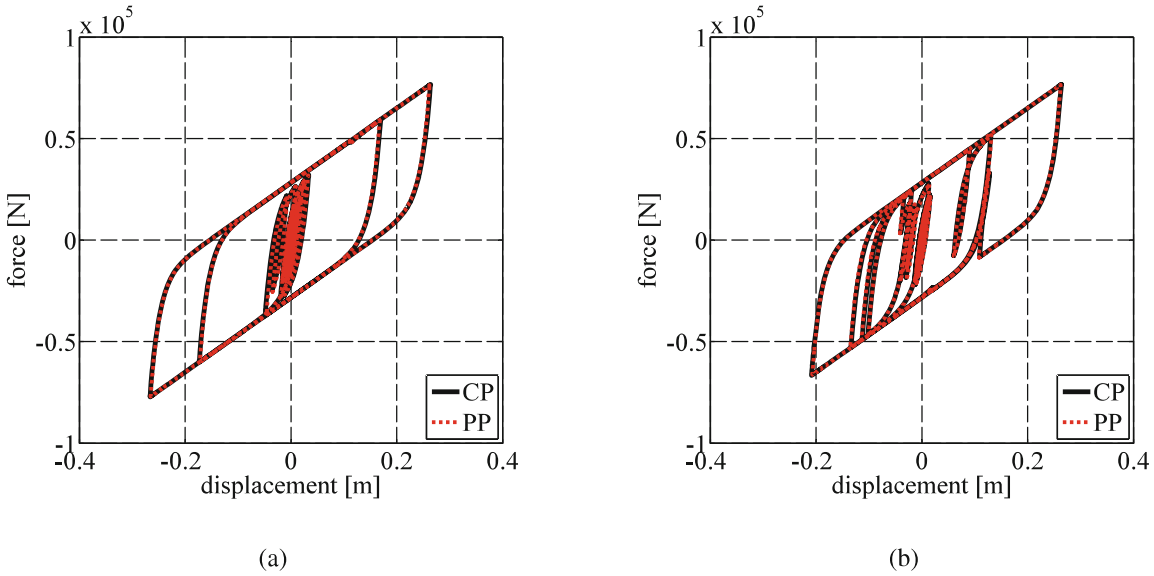

Fig. 3. Hysteresis loops of the Isolator 1 obtained along the (a) X and (b) Y directions.

6 Conclusions

We have presented a solution procedure to analyze seismically base-isolated structures with seismic isolators having a non-stiffening hysteretic behavior. Such a procedure combines a novel phenomenological model, obtained by specializing a more general class of models recently formulated by Vaiana et al. [24], and an explicit structure-dependent time integration method, obtained by specializing a family of explicit methods developed by Chang [15].

To show the accuracy and the computational efficiency of the proposed approach, nonlinear time history analyses have been performed on a base-isolated structure with elastomeric bearings. Specifically, the numerical results and the computational times obtained by the proposed strategy have been compared to those obtained by employing a conventional solution approach that combines the differential model proposed by Nagarajaiah et al. [7] with the widely used Newmark's constant average acceleration method adopted in conjunction with the pseudo-force iterative procedure.

The dynamic response of the analyzed structure, subjected to a bidirectional earthquake excitation, reveals that the accuracy of the presented strategy is very satisfactory since the numerical results closely match those predicted by the conventional one. In addition, the analyses results reveal that the computational burden required by the proposed strategy is reduced of three orders of magnitude with respect to that characterizing the conventional one; in particular, the total computational time percentage, *tctp*, of proposed approach is less than 0.50%.

In forthcoming papers, the proposed model will be extended to the two-dimensional case to better simulate the actual response of base-isolated structures subjected to bidirectional earthquake excitation [26]. Furthermore, the proposed model will be also adopted to analyze buildings with seismic devices [27] by using the concept of seismic response envelopes [28].

Acknowledgments. The present research was supported by the Italian Government, ReLUIS 2017 Project [AQ DPC/ReLUIS 2014–2018, PR2, Task 2.3] and PRIN 2015 Grants [2015JW9NJT-PE8, WP2, Task 2.1], which is gratefully acknowledged by the authors.

References

1. Vaiana, N., Sessa, S., Marmo, F., Rosati, L.: Nonlinear dynamic analysis of hysteretic mechanical systems by combining a novel rate-independent model and an explicit time integration method. Nonlinear Dyn. **98**(4), 2879–2901 (2019). https://doi.org/10.7712/120119.7304.19506
2. Pauletta, M., Cortesia, A., Pitacco, I., Russo, G.: A new bi-linear constitutive shear relationship for unbonded fiber-reinforced elastomeric isolators (U-FREIs). Compos. Struct. **168**(1), 725–738 (2017)
3. Vaiana, N., Sessa, S., Marmo, F., Rosati, L.: An accurate and computationally efficient uniaxial phenomenological model for steel and fiber reinforced elastomeric bearings. Compos. Struct. **211**(1), 196–212 (2019)
4. Kikuchi, M., Aiken, I.D.: An analytical hysteresis model for elastomeric seismic isolation bearings. Earthq. Eng. Struct. Dyn. **26**(2), 215–231 (1997)
5. Vaiana, N., Spizzuoco, M., Serino, G.: Wire rope isolators for seismically base-isolated lightweight structures: experimental characterization and mathematical modeling. Eng. Struct. **140**(1), 498–514 (2017)
6. Mokha, A., Constantinou, M.C., Reinhorn, A.M., Zayas, V.A.: Experimental study of friction-pendulum isolation system. J. Struct. Eng. **117**(4), 1201–1217 (1991)
7. Nagarajaiah, S., Reinhorn, A.M., Constantinou, M.C.: Nonlinear dynamic analysis of 3-D base-isolated structures. J. Struct. Eng. **117**(7), 2035–2054 (1991)
8. Charalampakis, A.E., Koumousis, V.K.: Identification of Bouc-Wen hysteretic systems by a hybrid evolutionary algorithm. J. Sound Vibr. **314**(3–5), 571–585 (2008)
9. Carboni, B., Lacarbonara, W., Auricchio, F.: Hysteresis of multiconfiguration assemblies of nitinol and steel strands: experiments and phenomenological identification. J. Eng. Mech. **141**(3), 1–16 (2014)
10. Brewick, P.T., Masri, S.F., Carboni, B., Lacarbonara, W.: Data-based nonlinear identification and constitutive modeling of hysteresis in NiTiNOL and steel strands. J. Eng. Mech. **142**(12), 1–17 (2016)
11. Strano, S., Terzo, M.: Accurate state estimation for a hydraulic actuator via a SDRE nonlinear filter. Mech. Syst. Signal Process. **75**(1), 576–588 (2016)
12. Newmark, N.M.: A method of computation for structural dynamics. J. Eng. Mech. Div. **85**(3), 67–94 (1959)
13. Greco, F., Luciano, R., Serino, G., Vaiana, N.: A mixed explicit-implicit time integration approach for nonlinear analysis of base-isolated structures. Ann. Solid Struct. Mech. **10**(1), 17–29 (2018)
14. Chang, S.-Y.: A new family of explicit methods for linear structural dynamics. Comput. Struct. **88**(11–12), 755–772 (2010)
15. Chang, S.-Y.: Family of structure-dependent explicit methods for structural dynamics. J. Eng. Mech. **140**(6), 1–7 (2014)
16. Bathe, K.: Finite Element Procedures. Prentice Hall, Upper Saddle River (1996)
17. Clough, R., Penzien, J.: Dynamics of Structures. McGraw-Hill, New York (1993)
18. Chopra, A.K.: Dynamics of Structures: Theory and Applications to Earthquake Engineering, 4th edn. Prentice Hall, Upper Saddle River (2012)

19. Losanno, D., Madera Sierra, I.E., Spizzuoco, M., Marulanda, J., Thomson, P.: Experimental assessment and analytical modeling of novel fiber-reinforced isolators in unbounded configuration. Compos. Struct. **212**(1), 66–82 (2019)
20. Madera Sierra, I.E., Losanno, D., Strano, S., Marulanda, J., Thomson, P.: Development and experimental behavior of HDR seismic isolators for low-rise residential buildings. Eng. Struct. **183**(1), 894–906 (2019)
21. Bouc, R.: Modele mathematique d'hysteresis. Acustica **24**(1), 16–25 (1971)
22. Wen, Y.K.: Method for random vibration of hysteretic systems. J. Eng. Mech. Div. **102**(2), 249–263 (1976)
23. Vaiana, N., Sessa, S., Paradiso, M., Rosati, L.: Accurate and efficient modeling of the hysteretic behavior of sliding bearings. In: 7th International Conference on Computational Methods in Structural Dynamics and Earthquake Engineering (COMPDYN 2019), Crete, Greece, 24–26 June 2019. https://doi.org/10.7712/120119.7304.19506
24. Vaiana, N., Sessa, S., Marmo, F., Rosati, L.: A class of uniaxial phenomenological models for simulating hysteretic phenomena in rate-independent mechanical systems and materials. Nonlinear Dyn. **93**(3), 1647–1669 (2018)
25. Rosenbrock, H.H.: Some general implicit processes for the numerical solution of differential equations. Comput. J. **5**(4), 329–330 (1963)
26. Losanno, D., Spizzuoco, M., Calabrese, A.: Bidirectional shaking table tests of unbonded recycled rubber fiber reinforced bearings (RR-FRBs). Struct. Control Health Monit. (2018). https://doi.org/10.1002/stc.2386
27. Nuzzo, I., Losanno, D., Caterino, N., Serino, G., Bozzo Rotondo, L.M.: Experimental and analytical characterization of steel shear links for seismic energy dissipation. Eng. Struct. **172**(1), 405–418 (2018)
28. Sessa, S., Marmo, F., Vaiana, N., Rosati, L.: A computational strategy for Eurocode 8 - compliant analyses of reinforced concrete structures by seismic envelopes. J. Earthq. Eng. 1–34 (2018). https://doi.org/10.1080/13632469.2018.1551161